Journal of Materials Chemistry

Cite this: *J. Mater. Chem.*, 2011, **21**, 16704

www.rsc.org/materials

FEATURE ARTICLE

# Metal nanomaterial-based self-assembly: Development, electrochemical sensing and SERS applications

**Shaojun Guo[ab] and Shaojun Dong*[ab]**

***Received 1st April 2011, Accepted 25th May 2011***
**DOI: 10.1039/c1jm11382h**

Metal nanomaterials (MNMs) have received considerable interest from different scientific communities due to their size, shape, composition and architecture-dependent chemical and physical properties. MNMs-based self-assembly techniques are often essential for creating new multi-dimensional assembly architectures, which are very important for revealing new or enhanced properties and application potentials. This feature article will focus on recent advances in MNMs-based self-assembly and their potential application in electrochemical sensor and surface enhanced Raman spectroscopy (SERS). First, new significant developments in different self-assembly strategies for constructing two-dimensional (2D) and three-dimensional (3D) MNMs-based arrays or superstructures will be summarized. Then, diversified assembling approaches to different types of hybrid or multifunctional nanomaterials containing MNMs will be outlined. The review next introduces some exciting new pushes for the use of nanoarchitectures produced through self-assembly techniques for applications in electrochemical sensors and SERS. Finally, we conclude with a look at the future challenges and prospects of the development of MNMs-based self-assembly.

[a]*State Key Laboratory of Electroanalytical Chemistry, Changchun Institute of Applied Chemistry, Chinese Academy of Sciences, Changchun, 130022, Jilin, China. E-mail: dongsj@ciac.jl.cn; Fax: +86-431-85689711*
[b]*Graduate School of the Chinese Academy of Sciences, Beijing, 100039, China*

## 1. Introduction

Self-assembly (SA) refers to a typical process by which nanomaterials or functional molecules spontaneously organize into ordered macroscopic architectures occurring at liquid–liquid,

**Shaojun Guo**

*Shaojun Guo was born in Shandong Province, China. He received his BS degree from Jilin University in 2005. Then, he moved to the Changchun Institute of Applied Chemistry as a PhD student and majored in analytical chemistry and material chemistry. He received his Ph.D. degree in 2010. He is currently a Postdoctoral research associate in the Department of Chemistry at Brown University. He has published over 80 papers in peer-reviewed international journals and his papers have been cited more than 1200 times giving him an h-index of 22. His scientific interests focus on carbon and metal nanomaterials for electrochemical, analytical and energy applications.*

**Shaojun Dong**

*Shaojun Dong is Professor of Chemistry at Changchun Institute of Applied Chemistry, Chinese Academy of Sciences, and an advisor in the State Key Laboratory of Electroanalytical Chemistry. She has been a Member of the Academy of Sciences of the Developing World since 1999. She has been on the Editorial and Advisory Board of six international journals: Chem. Commun., Biosens. Bioelectron., Electrochem. Commun., Sensors, Bioelectrochemistry, and Talanta. Her research interests concentrate on electrochemistry with interdisciplinary fields, such as chemically modified electrodes, nanomaterials and nanotechnology, bioelectrochemistry spectroelectrochemistry and biofuel cells. She has published over 800 papers in peer-reviewed international journals, their citations exceeding 15 000 giving her an h-index of 57.*

solid–liquid and gas–liquid interfaces either through direct interactions (*e.g.*, interparticle forces), or indirectly using a template or an external field.[1,2] When a SA process begins, the system's free energy trends to be minimized because SA is intimately associated with thermodynamic equilibrium.[1,2] At present, a central theme in nanoscience and nanotechnology is to advance the fundamental understanding of nanometre-sized object assembly, which is of great importance in finding new functional architectures with particular properties and functions.[3] Therefore, rational assembly strategies are usually required to construct the complex structures with novel collective properties and even pattern nanoscale building blocks for nanodevice fabrication.

As one of the hottest research fields, metal nanomaterials (MNMs) are of great importance in different application fields such as sensors, electronics, optics, biomedicine, catalysts and surface enhanced Raman spectroscopy (SERS) due to their size, shape, composition and architecture-dependent chemical and physical properties.[4] The integration of MNMs into one-dimensional (1D), 2D or 3D structures can lead to fundamentally interesting collective physical properties that can be manipulated by the control of the cooperative interactions between the MNMs. This is important for the organized assemblies of MNMs to optimize and extend their application potentials. For instance, chain-like Au nanoparticle (NP) assembly is particularly important for the fabrication of next-generation optoelectronic devices, owing to the collective properties that arise from coupling of optical properties of the individual Au NPs.[5] Au or Ag NP 2D arrays with tunable interparticle distances have very high SERS activity and reproducibility in comparison individual NPs.[6] To date, MNMs have been widely used as functional building blocks to fabricate multi-dimensional ordered assemblies for the development of high-performance nano-electronic, nano-optical and electrochemical devices based on different assembly techniques. For instance, the layer-by-layer (LBL) technique, which has good ability to fine-tune the composition of nanostructured films or nanocomposites, has been used to assemble MNMs on the solid substrate for creating advanced materials with enough structural flexibility to be tuned for specific applications such as electrochemical sensors.[7] The Langmuir–Blodgett (LB) assembly technique is also a good candidate for arranging a great number of MNMs with different size, shape and composition onto solid surfaces to construct functional interfaces for different applications.[8]

In this feature article, we will highlight some current efforts in developing new assembly techniques for constructing multi-dimensional ordered architectures and assembly architecture-based electrochemical sensing and SERS applications. Different assembly techniques leading to different-dimension nanoarchitectures by introducing MNMs into the assembly system will firstly be discussed. Then, assembly techniques for novel hybrid nanostructures with multi-functional properties or enhanced functions will be introduced. Besides discussing some new procedures for MNMs-based assembly architectures, the use of assembly architectures for electrochemical sensing and SERS applications will also be illustrated.

## 2. Assembly techniques for metal nanomaterials-based architectures

Rational assembly techniques are often essential for creating advanced materials with enough structural flexibility and functional assembly interfaces, which are important for revealing specific properties or applications.[9] MNMs with the variety of shapes and compositions provide the rich opportunities to combine their electronic, optical, and magnetic properties with other functional molecules for producing unique assembly architectures by manipulating the specific interactions, which leads to a new direction in the different application fields. At present, various assembly approaches have been employed to assemble MNMs in a controlled manner and to investigate the scope of potential applications.[1,2] These typical assembly approaches include LBL assembly, colloidal NP self-assembly techniques, solvent-induced evaporation, external field-driven assembly (*e.g.* LB technique, pressure), ion or small molecule or polymer induced assembly, self-assembly based on the integrity of different weak interactions and air–water or liquid–liquid interface assembly, *etc.* In this section, we will mainly highlight some recent achievements on typical techniques for constructing MNM-based 1D, 2D and 3D nanoarchitectures.

### 2.1 Solvent-induced evaporation strategy

Solvent-induced evaporation, which is essentially a far-from-equilibrium process, is a very common strategy for effectively controlling the 2D assembly of MNMs (MNMs are usually protected by hydrophobic ligands) because of the strong hydrophobic interaction of ligands that exists on the surface of MNMs.[10–20] In the well-known assembly system, spontaneous crystallization of metal nanostructures results from tuning the interparticle forces by optimization of solvent composition, evaporation rate, particle concentration, and particle surface chemistry. Sun *et al.* firstly reported the synthesis of monodisperse FePt NPs by reduction of platinum acetylacetonate and decomposition of iron pentacarbonyl in the presence of oleic acid (OA) and oleyl amine (OAm) stabilizers.[10] The as-prepared NPs could be easily self-assembled into 3D superlattices in the condition of solvent-induced evaporation. Later, in their OA-OAm system, some other well-defined MNMs-based 2D assembly architectures could also be easily obtained through the similar solvent-induced evaporation strategy. Some typical MNMs with different shapes, sizes and compositions such as Au NPs,[11] Au nanowires (NWs),[12] FePt nanocubes,[13] FePt nanorods (NRs),[14] Pt nanocubes[15] and even Pd/FePt core/shell NPs[16] could be facilely assembled into ordered 2D architectures (Fig. 1). In addition to the organic-phase system, aqueous-phase routes can be applicable to prepare high-quality MNMs-based 2D assembly architectures under the assistance of amphiphilic ligands. Typical work is from Xu *et al.*,[17] who developed a versatile seed-mediated growth method for selectively synthesizing single-crystalline rhombic dodecahedral (RD), octahedral, and cubic gold nanocrystals (NCs). They found that these monodisperse Au polyhedrons could be assembled into high-quality 2D assembly architectures. They also demonstrated that the present system could be used to assembly other metals such as Pd nanocubes into ordered 2D assembly architectures.[18] Although the above

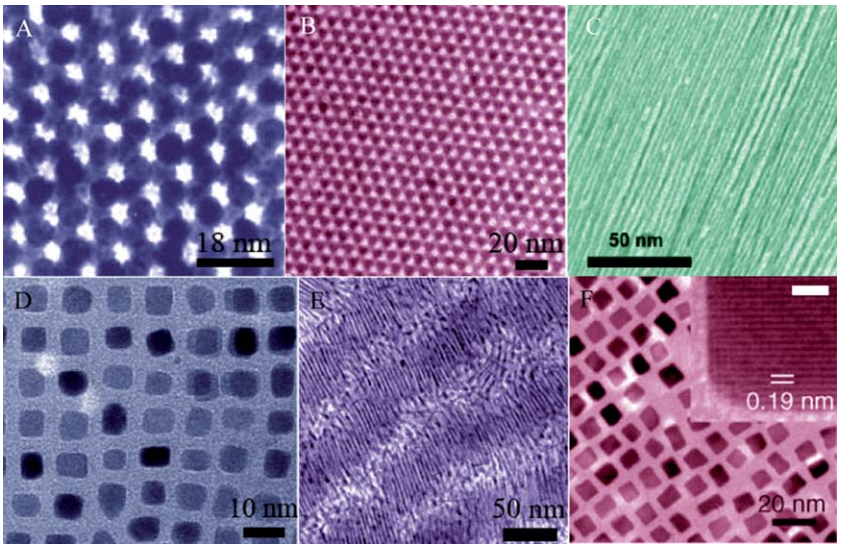


**Fig. 1** TEM images of FePt NPs (A) Au NPs (B), Au NWs (C), FePt nanocube (D), FePt NRs (E) and Pt nanocube (F). Reprinted from ref. 10 with from the American Association for the Advancement of Science. Reprinted from ref. 11 with permission from Springer Publishing Group. Reprinted from ref. 12, 13 with permission from the American Chemical Society. Reprinted from ref. 14, 15*b* with from Wiley-VCH.

system provides a good advantage for assembling high-quality MNMs into ordered 2D structures, it remains a great challenge to pattern the superlattices with comprehensive control over internal order and overall morphologies because of the statistical nature of drying-mediated self-assembly. Recently, Luo *et al.* successfully solved the issue and patterned such superlattices over a large area into a number of versatile structures with high degrees of internal order, including single-particle-width corrals and single particle-thickness microdiscs using DNA-protected gold NPs as a model (Fig. 2). Their assembly system involves moulding microdroplets containing the NPs and spatially regulating their dewetting process.[19,20] Later, they further used the DNA-based route to develop monolayered free-standing NP superlattices.[21] In an unconventional way, discrete, free-standing superlattice sheets with controlled inter-particle spacings and functional properties (plasmonic and mechanical) could be rationally controlled by adjusting DNA length. Most interestingly, the edge-to-edge inter-particle spacing for monolayered superlattice sheets could be tuned up to 20 nm, which is a much wider range than that obtained from alkyl molecular ligand protected gold NPs.

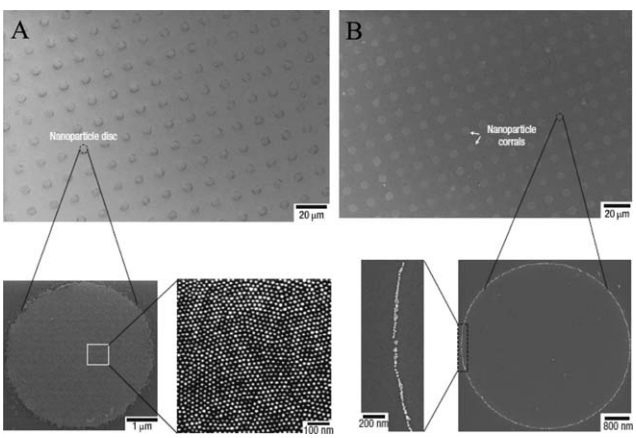


**Fig. 2** SEM images of monolayered superlattice microdiscs (A) and single-particle-width micro-corrals (B). Reprinted from ref. 19 with permission from Nature Publishing Group.

### 2.2 LBL assembly technique

LBL assembly is a powerful means for fabricating multilayer thin films with controlled architecture and composition, which usually involves the collective effect of some weak interactions (*e.g.* electrostatic interactions, hydrogen bonds, step-by-step reactions, sol–gel processes, molecular recognition and charge-transfer) between two assembling components.[7] Compared with conventional methods for constructing thin film, LBL assembly is simpler, more convenient and more universal and allows more precise thickness control at the nanoscale for the preparation of thin film.[22] MNMs are a kind of building block with interesting optical, electronic and magnetic properties and many potential applications in different fields. Using metal MNMs as building blocks of LBL for constructing different functional assembling interfaces are of great interest to scientists. Our group took the advantage of LBL techniques to develop a series of multi-component nanomaterial-based functional interfaces, which include thionine/gold NPs,[23] Au NPs/[tetrakis(*N*-methylpyridyl) porphyrinato]cobalt (CoTMPyP),[24] carbon nanotube (CNT)/thionine/gold NPs,[25] ferrocene-appended poly(ethyleneimine) (Fc-PEI)/gold NPs (Fig. 3),[26] CNT/Pt NPs,[27] ionic liquid-graphene/Pt NPs,[28] $Ru(bpyl)_3^{2+}$ doped silica sphere/Au NPs[29] and polymer/Au NRs multilayer films.[30] The resulting LBL functional interfaces exhibited high performance for the use in electrochemical sensors or SERS substrates, which will be discussed in the following application parts.

### 2.3 Langmuir-Blodget assembly

LB assembly is a good candidate for arranging a variety of metal nanostructures on solid surfaces, which is similar to the typical

 

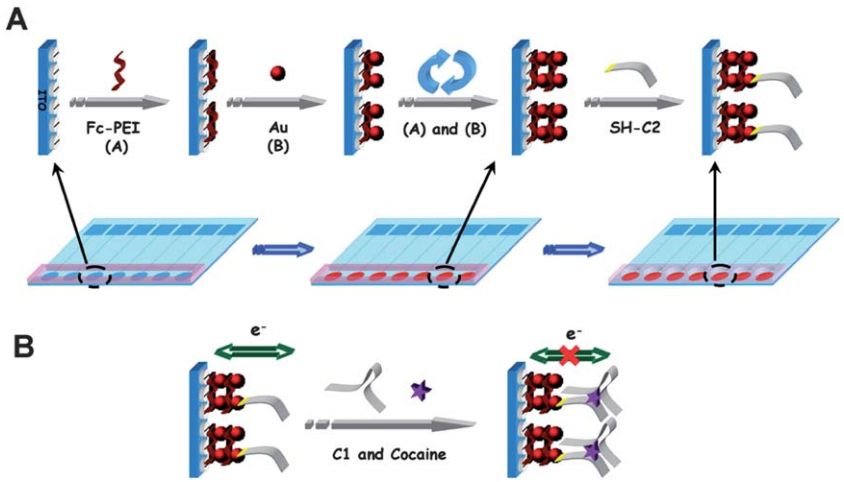


**Fig. 3** (A) Fabrication of the sensing interface and (B) Schematic routine for cocaine detection. Reprinted from ref. 26 with permission from the American Chemical Society.



assembly of amphiphilic molecules. In the MNMs-based LB systems, uniaxial compression of monolayers comprising MNMs floating on an aqueous subphase induces self-assembly and long-range packing over large surface areas.[31] Ordered 2D assembly architectures formed at the air/water interface could then be transferred onto solid or soft surfaces in their entirety, generally with high fidelity. Yang *et al.*[32] demonstrated the bottom-up assembly of polyhedral silver NCs into macroscopic 2D superlattices using the Langmuir–Blodgett technique. In their LB technique, the MNMs solution was spread at an air–water interface, thus forming an isotropic monolayer of floating MNMs. Their results show that interparticle spacing, density and packing symmetry could be easily controlled, which is important for allowing the tunability of the optical response over the entire visible range. Fig. 4 shows the typical scanning electron microscope (SEM) images of 2D superlattices composed of truncated cubes, cuboctahedra and octahedral Ag NCs. It is observed that truncated cubes tend to assemble face to face to form a square lattice (Fig. 4A) whereas cuboctahedra tend to form a rhombohedral unit cell (Fig. 4B). But, octahedra adopted a hexagonal lattice upon compression, lying flat on their triangular facets such that three NCs formed an interlocked triangle (Fig. 4C). Moreover, the present LB technique could also be extended to assemble other MNMs such as Pt nanocrystals[33] and Ag NWs.[34]

### 2.4 Liquid–liquid interface assembly

Liquid–liquid interfacial assembly strategies are of great interest for obtaining well-defined nanomaterial 2D arrays or nanomaterial assembly architectures. In the assembly system, hydrophilic NPs can be trapped at liquid–liquid interfaces by bringing the contact angle of particles with the interface close to 90 °C by introducing hydrophobic ligands into the surface of NPs or with the aid of amphiphilic solvent.[35] Wang *et al.* found that Au and Ag NPs with the terminal 2-bromopropionate group could render their contact angles at the water/oil interface close to 90 °C, driving them to the water/oil interface and to self-assemble into closely packed arrays.[35] Under the direction of this principle, the use of the specific inclusion of hydrophobic $CoPt_3$ NPs by cyclodextrins could direct them to self-assemble into macroscopic randomly close-packing monolayers at water/oil interfaces.[36] Interestingly, Vanmaekelbergh *et al.*[37] showed that ethanol as an amphiphilic molecule could force the contact angle of citrate-stabilized hydrophilic Au NPs with a heptanes–water interface close to 90 °C, which caused these NPs to form a 2D monolayer thin film. However, in many cases the above NP films assembled at liquid–liquid interfaces were found to be randomly distributed and did not form an ordered structure. Later, Sun *et al.*[38] reported a universal approach for the self-assembly of hydrophilic NPs (Au, Ag and silica) into ordered NP thin films at toluene–water interfaces by the use of ethanol for subtly controlling the interfacial tension of the two phases (Fig. 5). Following this work, Wang's group[39] demonstrated a modified process that the water–alcohol interface could be directly used to form macroscopic, dried, freestanding monolayer films of the NPs without the aid of sacrificial supports or molecular glues. The present approach allowed the growth of dry freestanding films of Au NP monolayers as large as several square centimetres. Moreover, a liquid–liquid interface assembling strategy was employed to construct a uniform 3D raspberry-like gold sphere[40] or 1D rectangular silver NRs arrays on a solid substrate.[41] The as-prepared rectangular silver NRs arrays were excellent SERS substrates with high activity, stability, and reproducibility.

### 2.5 Pressure-driven assembly

External force is also utilized to engineer MNMs-based assembly, to fabricate 1D metallic nanostructures and even to form ultrahigh-density ordered 1D or multi-dimensional nanostructure arrays. In the force-driven assembly system, 2D ordered films of metal NPs with a face-centered cubic (fcc) mesophase were compressed using a diamond anvil cell with different pressures, then the pressure was gradually released back to ambient pressure.[42,43] Under proper pressure, the NPs could be connected with each other to form multi-dimensional assembly architectures. Fan *et al.* demonstrated such a pressure-directed assembly for the preparation of a new class of chemically and mechanically stable gold assembly nanostructures through

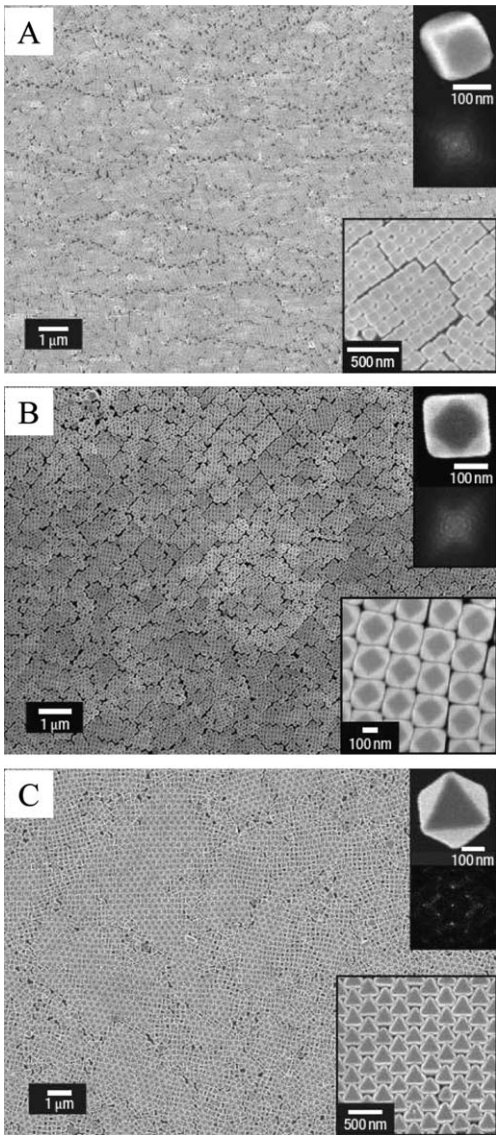


**Fig. 4** Novel superlattice architectures composed of different polyhedral building blocks. (A) Truncated cubes, (B) cuboctahedra and (C) octahedra Ag NCs. Reprinted from ref. 32 with permission from Nature Publishing Group.

high pressure-driven sintering of Au NP assemblies at room temperature.[42,43] They found that under a hydrostatic pressure field, the unit cell dimension of a 3D ordered NP array could be reversibly manipulated allowing fine-tuning of the interparticle separation distance in 2D or 3D NP assemblies. Fig. 6 shows the typical transmission electron microscopy (TEM) images of gold NP assembly architectures, which are organized in a periodic, ordered mesostructure. After the pressure was increased to 12.4 GPa and then released to ambient pressure, 3D ordered, interconnected, branched gold nanoskeleton were obtained (Fig. 6A, B).[42] However, after release of the pressure from 13 GPa to ambient pressure, the result was different. In this case, the ordered fcc NP superlattice could be converted into an ordered NW array, which consisted of individual Au NWs with hexagonal close packing (Fig. 6C–F).[43]

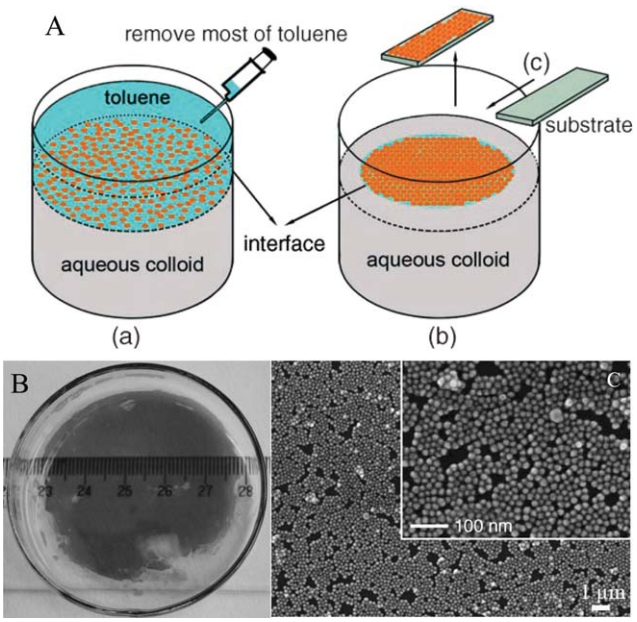


**Fig. 5** (A) Schematic representation of the formation and transfer of a monolayer film (MLF). The MLF formed initially was incompact and disordered (a); NPs assemble into a close-packed MLF after most of the toluene has been removed (b); the MLF was transferred onto a solid substrate (c). (B) Photograph of an Au NP film deposited on the bottom of a Petri dish. Each mark on the ruler represents 1 mm. (C) SEM image of MLFs of Au NPs. Reprinted from ref. 38 with permission from Wiley-VCH.

### 2.6 Molecular interaction-directed self-assembly of metal nanoparticles

Recently, self-assembly of oppositely charged, nanoscopic metal NPs into larger, ordered architectures is an attractive avenue to get new types of supracrystals. The formation of these supracrystals results from the change in electrostatic interactions in the nanoscopic regime, where the thickness of the screening layer becomes commensurate with the dimensions of the assembling particles. Actually, in the binary assembly process, smaller, charged NPs could stabilize larger NPs, which would facilitate the form of well-defined supracrystals. Grzybowski and co-workers demonstrated the first example on electrostatic self-assembly of oppositely charged, nearly equally sized metallic NPs of different types into large 3D diamond-like crystals, which was mediated by screened electrostatic interactions.[44,45] They could easily control the overall crystal morphologies including octahedral, truncated tetrahedral, truncated and twinned octahedral, and triangular structures through changing the experimental parameters (Fig. 7). They also showed that through increasing the proportion of NPs of one polarity, it was possible to terminate the self-assembly process at various crystal stages and thus effectively control the supracrystals' sizes and solubilities.[46] Moreover, electrostatic interactions could be further employed to assemble anisotropic metallic NPs such as Au nanotriangles (NTs) into ordered monolayer and multilayer structures.[47] The remarkable feature of this method is that the electrostatic repulsions could weaken the strong van der Waals attractions between the flat faces of the triangles and effectively serve as a "molecular lubricant", which

 

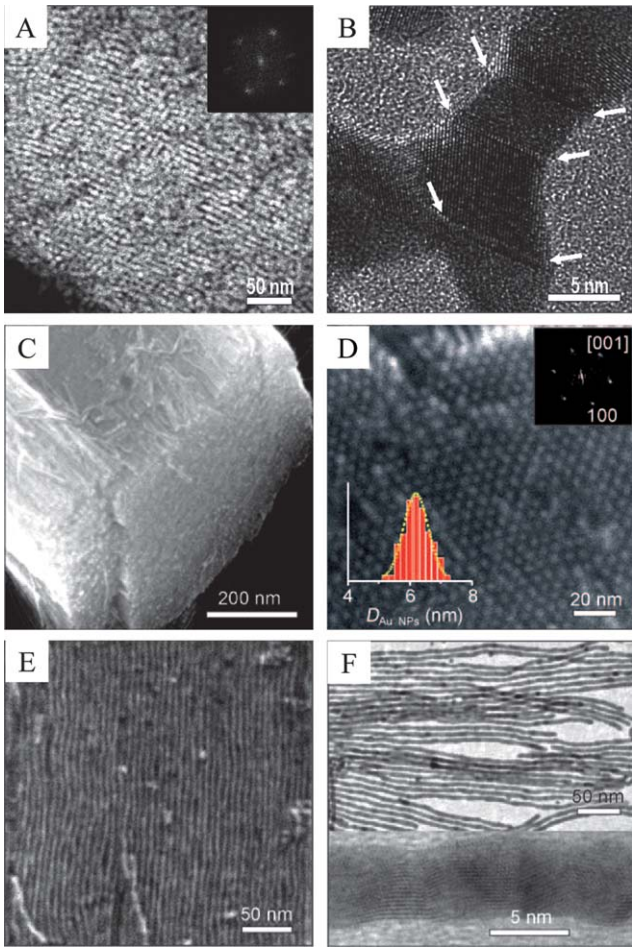


**Fig. 6** A, B: The scanning transmission electron microscopy (STEM) dark field images of 3D gold networks after releasing pressure from 12.4 GPa to ambient pressure. Reprinted from ref. 42 with permission by American Chemical Society. C–F: SEM images of gold NW ordered array along different directions after release of the pressure from 13 GPa to ambient pressure. Reprinted from ref. 43 with permission from Wiley-VCH.

allowed the NTs to fine-tune their mutual orientations, thus leading to a well-defined NT array.

Cooperative two-point electrostatic interaction,[48] covalent bonding,[49] antibody–antigen or biotin–streptavidin,[50] DNA base interaction,[51] electric dipole–dipole interaction,[52] and small molecule-mediation,[53] *etc.* could also be used to regulate the assembly of MNMs under the optimal conditions. For instance, Yan *et al.*[48a] found that gold NRs, nanospheres, and bipyramids could be assembled into three types of necklace structures such as NR–NR, NR–nanosphere and bipyramid–nanosphere using glutathione and cysteine as linkers based on the cooperative two-point electrostatic interaction (Fig. 8A). Chen *et al.*[49] showed that covalent bonding could promote the formation of stoichiometry-controlled hetero-assembly of gold NPs in the solution-based assembly system (Fig. 8B, C). DNA is an interesting functional molecule for posing as both the scaffold and the linker for construction of the MNMs-based assembly architectures because of their inherent molecular recognition properties. A recent significant contribution was given by Yan *et al.*,[51f] who demonstrated that through the attachment of single-stranded

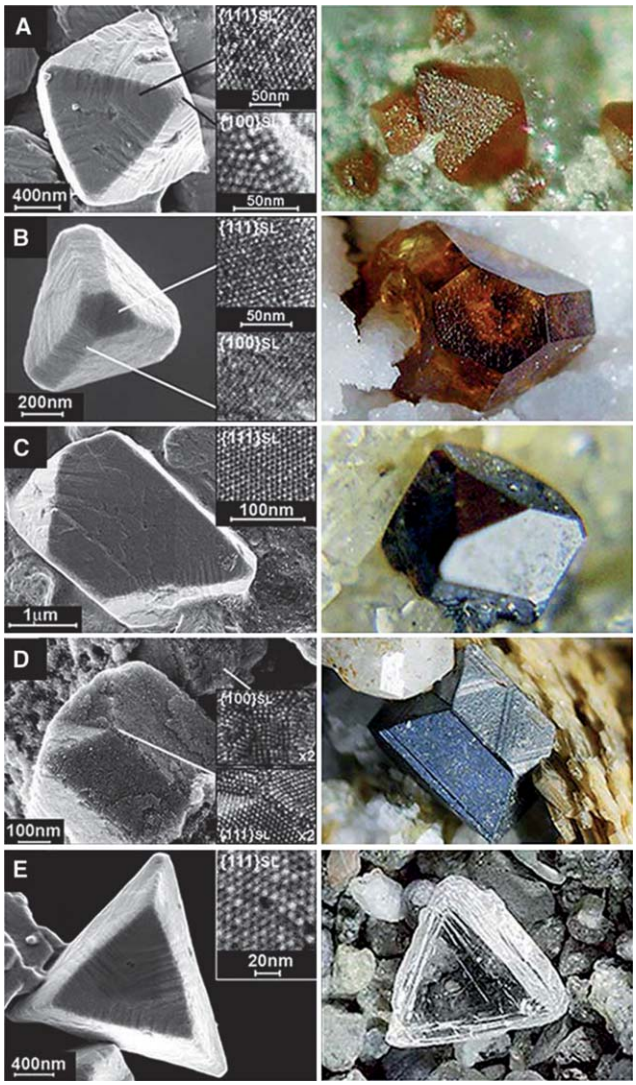


**Fig. 7** Different morphologies of the Au–Ag supracrystals (left column) and their macroscopic sphalerite (SL) (A to D) and diamond (E) counterparts (right column). (A) Octahedron; insets show $\{111\}_{SL}$ and $\{100\}_{SL}$ faces. (B) Cut tetrahedron; insets show $\{111\}_{SL}$ and $\{100\}_{SL}$ faces from cut top and from cut edge, respectively. (C) Octahedron with two triangular faces cut; inset shows the $\{111\}_{SL}$ face. (D) Twinned octahedron; insets magnify $\{111\}_{SL}$ faces at the location of twinning and the $\{100\}_{SL}$ face of a broken neighboring crystal. (E) Truncated tetrahedron; inset shows top view of the $\{111\}_{SL}$ face. Reprinted from ref. 44 with permission by the American Association for the Advancement of Science.

DNA to gold NPs, nanotubes of various 3D architectures containing gold NPs could form, ranging in shape from stacked rings to single spirals, double spirals, and nested spirals (Fig. 8D). The above contributions indicate that by engineering molecular interactions, one should be possible to effectively control the MNMs-based assembly for different functional architectures.

## 3. Self-assembly strategy for multi-component hybrid nanostructures

Self-assembly strategy can provide a convenient and versatile process for the controlled preparation of multi-component

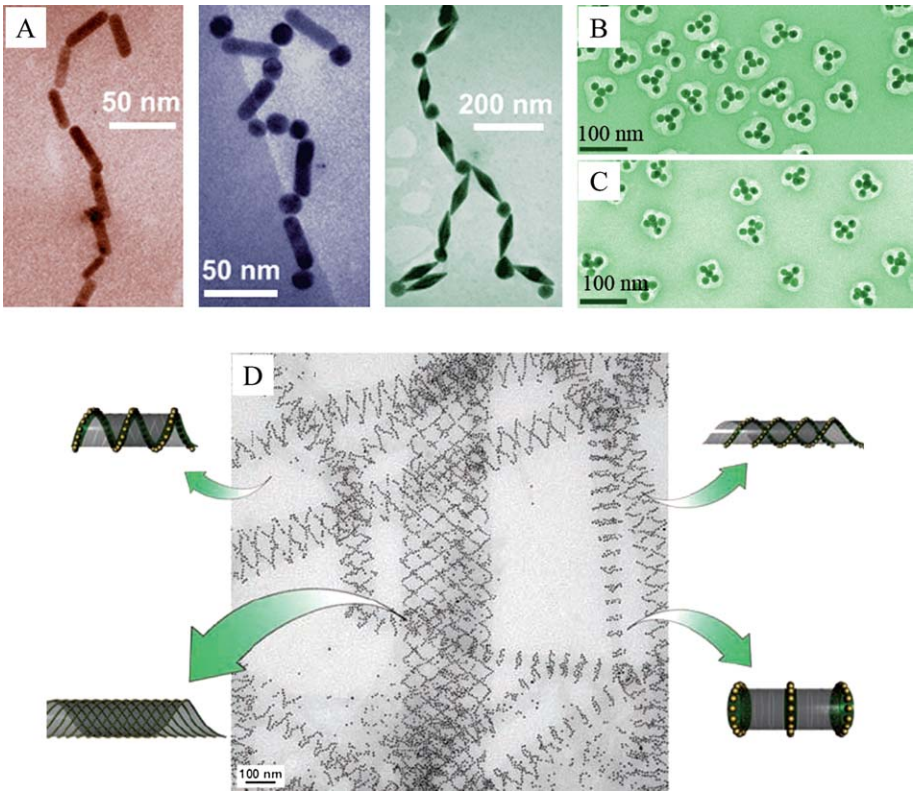


**Fig. 8** A: TEM images of Au NRs, bipyramid and nanospheres assembled into chain structures. Reprinted from ref. 48*a* with permission from the Royal Society of Chemistry. B, C: TEM images of $AB_3$ and $AB_4$ Au NPs assemblies. Reprinted from ref. 49 with permission from Nature Publishing Group. D: The design of a DNA tile system for the formation of a variety of tubular structures carrying 5-nm Au NPs. Reprinted from ref. 51*f* with permission from the American Association for the Advancement of Science.

hybrid nanoarchitectures with enhanced or multifunctional properties based on different interactions. Through self-assembly techniques, different nanoscale materials can be combined into one entity that simultaneously exhibits novel optical, electronic, and magnetic properties, or even enhanced properties. Inspired by this, we employed self-assembly strategies for constructing a series of CNTs/metal hybrid nanostructures using very homogeneous $TiO_2$ or silica as a linker,[54–56] magnetic NPs/metal hybrid architectures using 3-aminopropyltrimethoxysilane (APTMS) as a linker,[57] graphene/Pt-on-Pd bimetallic nanodendrite hybrids[58] and graphene/Au NPs hybrids using polymer as a linker.[59] For instance, we have developed a simple, efficient, economical, and general approach to construct diverse multifunctional $Fe_3O_4$/metal hybrid nanostructures using APTMS to functionalize $Fe_3O_4$ nanospheres.[57] High-density Au NPs could be supported on the surface of superparamagnetic $Fe_3O_4$ spheres and used as seeds to construct Au shell-coated magnetic spheres displaying near-infrared (NIR) absorption, which may make them promising in biomedical applications. High-density flower-like Au/Pt hybrid NPs could be supported on the surface of $Fe_3O_4$ spheres to construct recycled hybrid nanocatalysts with high catalytic activity towards the electron-transfer reaction between potassium ferricyanide and sodium thiosulfate (Fig. 9). High-density Ag or Au/Ag core/shell NPs could also be supported on the surface of $Fe_3O_4$ spheres and exhibited high SERS activity, which may possibly be used as an optical probe with magnetic function for application in high-sensitivity bioassays. Other interesting examples include the preparation of 1D gold NP arrays by electrostatically directed organization using polypeptide self-assembly,[60] assembly of CNT-metal NPs hybrids using biointerfaces,[61] the synthesis of porous gold NP-$CaCO_3$ hybrid microspheres,[62] and the design of CNTs/Pt nanocube hybrids by a noncovalent LBL functionalization method, *etc.*[63]

Molecular engineering of nanomaterials is an attractive approach for hierarchical organization of different types of nanomaterials to construct multifunctional assembly architectures containing MNMs. For instance, Hyeon and coworkers[64] designed a muti-step strategy for getting multifunctional nanocomposites by subsequent assembly of CdSe/ZnS quantum dots (QD) or Au or Pd NPs on the magnetite NP-bearing silica spheres. The general synthetic procedure for multifunctional NP/silica sphere assemblies is shown in Fig. 10. First, uniformly sized

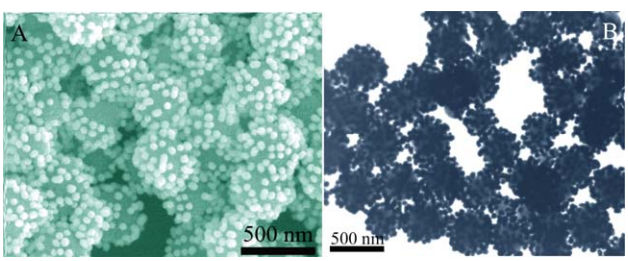


**Fig. 9** SEM (A) and TEM (B) images of $Fe_3O_4$/Au-Pt NPs Hybrids. Reprinted from ref. 57 with permission from Wiley-VCH.

silica spheres were prepared by the Stöber method and then functionalized with amino groups by treatment with APTMS. Second, the $Fe_3O_4$ NPs were assembled on the surfaces of the amino-functionalized silica spheres, followed by assembling the CdSe/ZnS QDs, Au or Pd onto the uncovered surface of $SiO_2$ spheres to give multifunctional assemblies. The as-obtained multifunctional silica spheres exhibited a combination of magnetism and luminescence (CdSe/ZnS), surface plasmon resonance (Au) or catalysis (Pd). The present assembly process could also be extended to prepare magnetic and optical nanohybrids based on $Fe_3O_4$ and gold nanoshells, both of which were coated on the surface of monodisperse silica nanospheres.[65] In addition to silica, poly-L-histidine (PLH) has been proven to be a good linker for constructing well-defined multifunctional assembly architectures. The typical work is from Gao *et al.*,[66] who demonstrated the first successful examples on the preparation of gold-shell-encapsulated QDs by means of peptide-templated shell growth. The key to QD-gold core-shell nanocomposites with controlled internal distance was to first coat lipid-stabilized water-soluble QDs with a layer of PLH. Then, the histidine groups of PLH on the surface of QDs were capable of immobilizing $Au^{3+}$ ions at very high packing density for the deposition of thin and smooth gold shells. And, the spacing between a QD core and an ultrathin gold shell with nanometre precision could be easily achieved through a LBL assembly process (Fig. 11A). Fig. 11B shows the representative TEM images of the QD-gold core-shell NPs. It is observed that the shell thickness was about 2–3 nm, with a transparent gap of about 3 nm observed between the core and shell. Interestingly, the as-prepared bifunctional QD-Au core/shell nanohybrids exhibited high quantum yield (39%), high photostability against photobleaching, and strong surface plasmonic resonance (SPR) absorption, all of which are important for multimodal bioimaging in the biomedical fields. Later, they further extended the present assembly system to prepare a new class of iron oxide-gold core-shell NPs, which an important multifunctional materials offering contrast for magnetic resonance imaging, scattering-based imaging and magnetomotive photoacoustic imaging.[67]

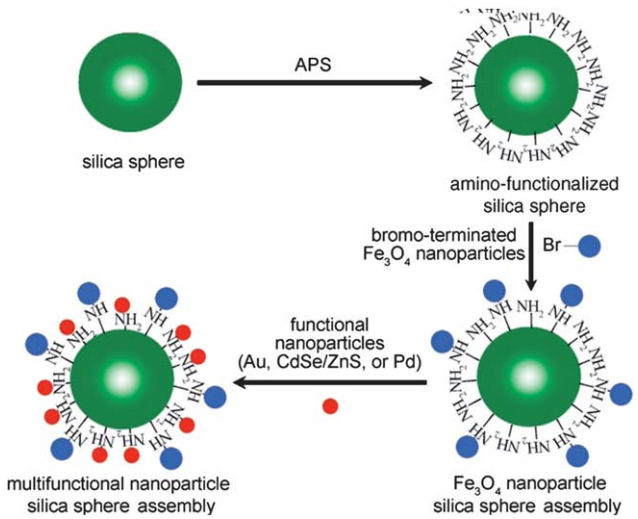


**Fig. 10** Synthetic procedures to obtain multifunctional NPs/silica sphere assemblies. Reprinted from ref. 64 with permission from Wiley-VCH.

## 4. Self-assembly metal nanostructures for electrochemical sensing and SERS applications

### 4.1 Electrochemical sensors

Electrochemical techniques promise rapid, simple, and low-cost detection and also allow device miniaturization for samples with a very small volume. For the electroanalytical chemist, it is primarily interesting how electrochemical sensing platforms can be designed for improving the sensitivity and selectivity by using inorganic nanomaterials as the enhanced or label elements. In all of the different nanomaterials, MNMs provide better opportunities for constructing high-performance electrochemical sensing interfaces because of their advanced advantages such as high conductivity, good biocompatible and good chemical stability. At present, various methodologies have been used for the tailoring of MNMs on electrode surfaces for electrocatalytic applications, which include anchoring by electrostatic interaction, covalent linkage and electrochemical deposition, *etc.*[68] Among them, MNMs-based self-assembly is a very interesting technique for building new electrochemical functional interfaces. For instance, our group[69] reported a novel sol–gel process combined with assembly technique for the fabrication of a horseradish peroxidase biosensor. In the electro-sensing platform (Fig. 12), a cleaned gold electrode was first immersed in a hydrolyzed (3-mercaptopropyl)-trimethoxysilane (MPS) sol–gel solution to assemble 3D silica gel, and then gold NPs were chemisorbed onto the thiol groups of the sol–gel network. The resulting biosensor exhibited a fast amperometric response to $H_2O_2$ with a low detection limit. Later, Raj's group extended the present system to construct a nonenzymatic electrochemical sensor for the detection of glucose by only using Au NPs self-assembled on a 3D MPS functionalized silicate network.[70] Our group has also shown[71] that the partial sulfonated (3-mercaptopropyl)-trimethoxysilane sol–gel film (PSSG) could act as both an ion exchanger for the immobilization of $Ru(bpy)_3^{2+}$ and a matrix to assembly gold NPs (electronic accelerating component). The as-prepared AuNPs/PSSG/$Ru(bpy)_3^{2+}$ film allowed the sensitive detection of nicotinamide adenine dinucleotide (NADH) as low as 1 nM based on $Ru(bpy)_3^{2+}$ electrochemluminesence (ECL) system. Aptamer is a kind of *in vitro* selected functional DNA or RNA sequences that can bind a wide range of non-nucleic acid targets such as small molecules, ion, proteins, and even cells. By assembly techniques for building sandwiched structures on the surface of electrode using MNMs as label or magnified components, a series of high-performance electrochemical sensors based on different sensing strategies can be developed for the detection of different targets.[72–81] For instance, our group developed a sensitive amplified electrochemical impedimetric aptasensor for thrombin, which has a sensitive detection limit of 0.02 nM, with a linear range of 0.05–18 nM.[72] Later, we extended the above system to develop a sensitive surface plasmon resonance (SPR) sensor for the detection of $Hg^{2+}$ in aqueous solution by using a thymine (T)-rich, mercury-specific oligonucleotide probe and Au NPs-based signal amplification.[73] Different to our system, Willner *et al.*

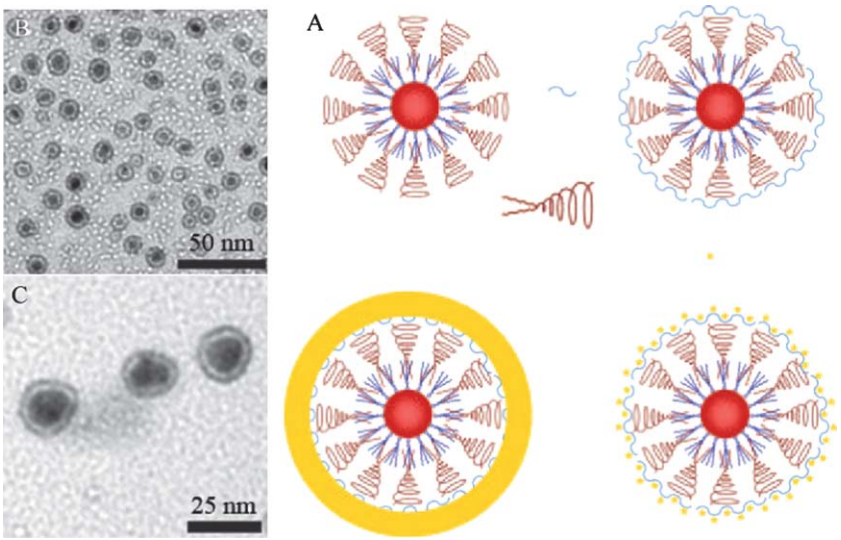


**Fig. 11** A: Schematic of gold-shell-encapsulated QDs. Hydrophobic QDs coated with trioctylphosphine oxide (molecules on QD surface, blue) were solubilized with a lipid-PEG-COOH conjugate (purple). The water-soluble QDs were then coated with PLH (blue curves) for immobilization of $Au^{3+}$ ions at high density. Addition of a mild reducing agent, hydroxylamine, led to gold nucleation on the PLH template and formation of a thin gold shell. B, C: TEM images of gold-shell-encapsulated QDs at different magnifications. Reprinted from ref. 66 with permission of Nature Publishing Group.

found that nucleic acid-functionalized Pt NPs could act as catalytic labels for the amplified electrochemical detection of DNA hybridization and aptamer/protein recognition.[74]

The LBL self-assembly technique is another powerful method to fabricate functional electrochemical sensing interfaces, due to its simplicity, controllability and versatility in combination with high quality and uniform coating. By a LBL self-assembled Fc-PEI/Au NPs multilayer with on an indium tin oxide (ITO) array electrode, our group constructed a label-free electrochemical aptasensor for detection of cocaine. As show in Fig. 3, the Fc-PEI and Au NPs were assembled on the electrode surface *via* electrostatic interactions. Then, cocaine aptamer fragments, SH-C2, were covalently labeled onto the outermost Au NP layer. When the target cocaine and cocaine aptamer C1 were present simultaneously, the SH-C2 layer hybridized partly with C1 to bind the cocaine, which led to a decreased differential pulse voltammetry (DPV) signal of Fc-PEI. Based on the principle, the lowest detectable concentration of cocaine could reach to 0.1 μM with the linear detection range extending up to 38.8 μM.[26] We also presented a LBL assembly process to assemble thionine cross-linked CNTs with Au NPs to form multilayer films for constructing NADH and glucose biosensors. Interestingly, it was found that the enhanced photovoltaic effect of thionine caused by both CNTs and Au NPs could strengthen the bio-electrocatalytic processes, thus leading to an increase in sensitivity of around 7 fold with the light irradiation than that in the dark.[25]

In addition, MNMs-based assembly aggregates are important nanocomposite materials to enrich a great number of $Ru(bpy)_3^{2+}$ molecules for enhancing the ECL performance using MNMs as

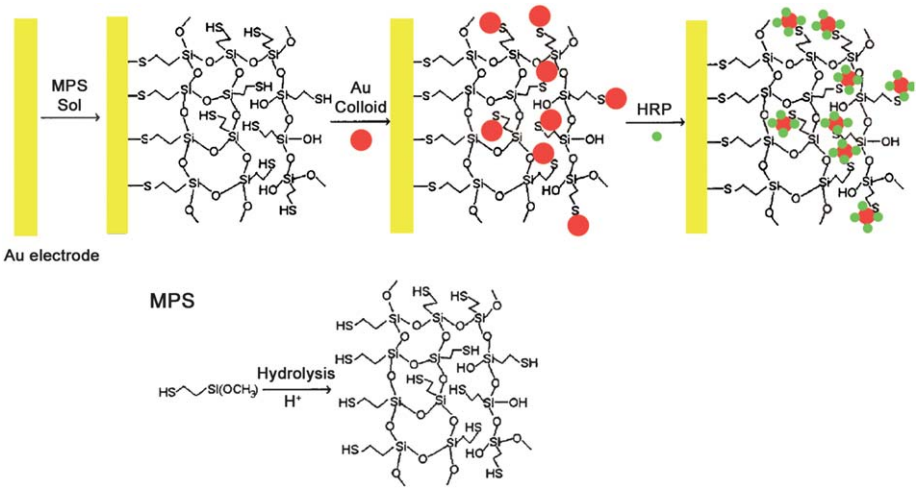


**Fig. 12** Hydrolysis of MPS and the stepwise biosensor fabrication process. Reprinted from ref. 69 with permission from the American Chemical Society.

 

an electronic accelerating component.[82–84] Several important examples are mainly from our group. For instance, the electrostatic interactions between citrate-capped Au NPs and Ru(bpy)$_3$Cl$_2$ in aqueous medium have been used to fabricate Ru(bpy)$_3^{2+}$-Au NP assembly aggregates, which exhibited excellent ECL behavior, and hence held great promise for solid-state ECL detection in capillary electrophoresis (CE) or a CE microchip (Fig. 13).[82] Then, the Pt NPs protected by 3-thiophenemalonic acid could be used as enriched materials to assembly Ru(bpy)$_3^{2+}$ into large aggregates. Directly placing such aggregates on bare ITO electrodes produced stable films exhibiting excellent electrochemiluminescence behavior.[83]

### 4.2 Self-assembly metal nanostructures for SERS applications

Surface-enhanced Raman scattering (SERS) is a phenomenon in which the Raman scattering cross-sections of molecules residing on or near the surfaces of certain MNMs are enhanced by factors up to $\sim 10^{14}$.[85] In particular, one can get a very large enhancement when the gap between MNMs is less than 10 nm, depicted by hot spots (highly localized regions of large local field enhancement).[86] At present, based on its high sensitivity, SERS has been shown to be a useful and powerful tool in detecting different targets with high speed and great specificity. However, two important issues should be adequately taken into consideration in order to accurately detect the target. (The first is SERS activity and the second is related to SERS reproducibility.) Therefore, how to achieve a large, reliable, stable, uniform, and reproducible SERS signal spanning a wide dynamical range is very important for semi-quantitative or quantitative sensing applications and has been a tremendous challenge. To a large extent, silver and gold NPs of various shapes and sizes or even aggregates induced by inorganic salt have been used as high-efficiency SERS substrates, but these substrates have poor reproducibility due to the challenge posed by inefficient control of the aggregation process.[87] Controlled self-assembly of nanostructured materials provides a feasible project for obtaining a SERS substrate with high activity and reproducibility. Several typical examples are shown here. Halas'7s group described a convenient and cost-effective chemical approach to fabricate highly ordered Au NP arrays with sub-10-nm spacing between adjacent NPs through employing solvent-evaporation strategy, which exhibited high, stable, and reproducible SERS activity (Fig. 14A).[6] LB technique was used to assemble monolayers (with areas over 20 cm$^2$) of aligned silver NWs, serving as excellent SERS substrates with large electromagnetic field enhancement factors and good reproducibility.[34] Despite the obvious advantages, one of the issues about the above LB technique for reproducible SERS substrates is that it needed special equipment and a complex operating process. A liquid–liquid assembly strategy has been a good alternative for constructing uniform MNM-based arrays such as Ag NRs and Au NRs on a solid substrate which could be used as SERS substrates with high activity, stability, and reproducibility.[41] Recently, a vertical deposition self-assembly method has been used to assemble monodisperse Au NCs into 2D and 3D superstructures. Each layer of the as-prepared superstructures

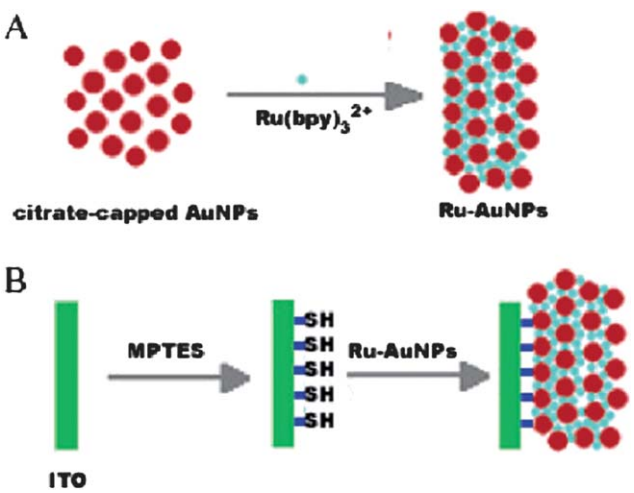


**Fig. 13** Scheme illustrating (A) the formation of Ru–Au nanocomposite in aqueous medium due to electrostatic interactions between Ru(bpy)$_3^{2+}$ and citrate-capped Au NPs and (B) the immobilization of Ru-AuNPs on a sulfhydryl-derivated ITO electrode surface. Reprinted from ref. 82 with permission from the American Chemical Society.

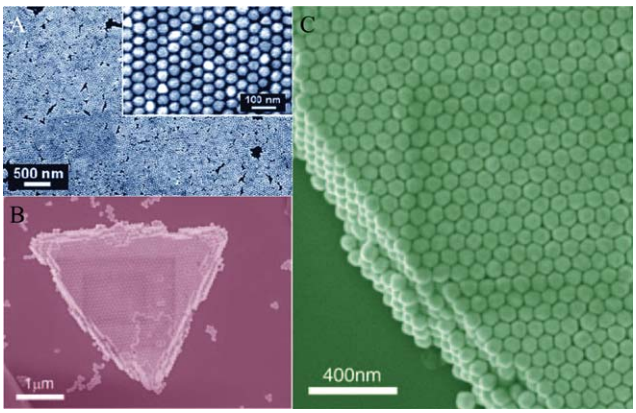


**Fig. 14** (A) SEM image of the monodisperse Au NP array. Reprinted from ref. 6 with permission from the American Chemical Society. (B, C) SEM images of self-assembled RD Au nanocrystals on silicon substrates. B: single triangular superstructure; C: magnified image of a triangular superstructure. Reprinted from ref. 88 with from Wiley-VCH.

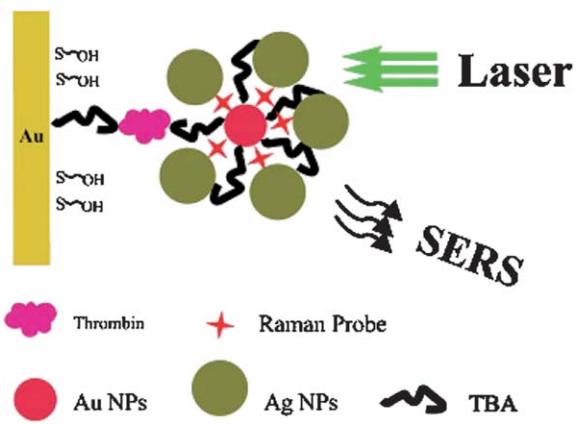


**Fig. 15** Schematic illustration of the fabrication process of SERS aptasensor for protein recognition. Reprinted from ref. 90 with permission from the Royal Society of Chemistry.

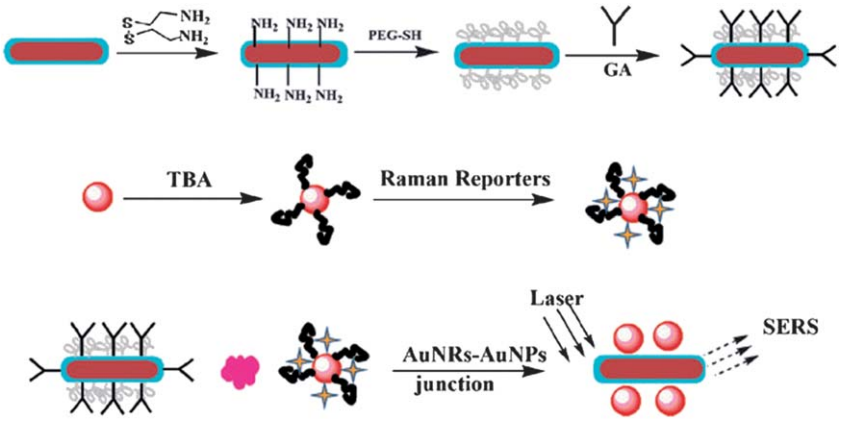


**Fig. 16** Fabrication of Au NR–Au NP junctions for protein detection-a schematic representation. Reprinted from ref. 93 with permission from the Royal Society of Chemistry.



was a triangle, 1–6 μm in size, which also exhibited high SERS activity and reproducibility as it had many hotspots and a uniform structure (Fig. 14B, C)[88]

The remarkable sensitivity of MNM-based SERS substrate suggests the possibility of basing ultrasensitive chemical/biological sensing techniques on SERS and has led to a number of ingenious strategies for developing a reliable SERS sensing platform.[89–96] For instance, Reich's group described a label-free SERS sensing platform for the unambiguous detection of single-stranded DNA by self-assembling probe-tethered Ag NPs to a "smooth" Ag film using the complementary target species.[89] Our group reported an assembly technique for developing novel SERS aptasensors for protein recognition based on Au NPs labeled with aptamers and Raman reporters using a sandwiched model followed by Ag NPs amplification, which opened a new way for protein recognition of high sensitivity and selectivity. As shown in Fig. 15, due to the strong electromagnetic coupling effect produced by the hot spots residing in the Au NPs and Ag NPs, the aptasensor has high sensitivity with the detection limit of 0.5 nM.[90] The present sandwiched strategy has been modified to achieve a heterogeneous or even multiplexed assay for protein detection with high sensitivity and selectivity using silver-NPs dimers held together by a Raman reporter instead of Au NPs protected by Raman reporter.[91,92] A multicomponent nanostructure comprising of gold NR–NP composites in the form of sandwiched model was also fabricated by assembly technique to detect thrombin with the detection limit of 220 pM. As shown in Fig. 16, the strong electromagnetic coupling resonance at the NR–NP junction of these probes was important for constructing the present highly sensitive SERS aptasensors.[93]

## 5. Conclusions and outlook

In summary, the examples covered in this feature article highlighted recent important advances in diverse assembly strategies for advanced MNMs-based assembly architectures. These typical assembly techniques include solvent-induced evaporation strategy, LBL assembly technique, LB assembly, liquid–liquid interface assembly, pressure-driven assembly and molecular interaction-directed self-assembly, *etc.* The directed self-assembly also provides new tools for a tailored, bottom up approach to the designed synthesis of MNMs-based multi-component or multifunctional hybrid nanomaterials. Particularly, MNMs-based self-assembly strategies endow enrich opportunities for constructing high-performance electrochemical and SERS sensing platform. Despite these important achievements, while there is certainly more fundamental work to be done to explore new assembly techniques for novel assembly micro/nanoarchitectures. In particular, at present, the formation of most assembly architectures can be modeled and justified only *a posteriori*, and there are few examples of assembly systems in which the assembly process can be predicted or conducted in compliance with people's requirements. Thus, understanding the essences of interaction forces acting between metal nanoscopic components and underlying their self-assembly into larger structures from both experimental and theoretical viewpoints is very important for creating new assembly architectures and understanding the effects of assembly structure on properties and functions and even revealing new properties and functions. The ultimate goal for MNMs-based self-assembly is to develop low-cost, high-throughput and accurate strategies for the preparation of MNMs-based assembly architectures with desirable fine structure, which will greatly advance the development of nanoscience and nanotechnology, especially applications in high-performance electrochemical and SERS sensors.

## Acknowledgements

This work was supported by National Natural Science Foundation of China (Nos. 20935003, 20820102037, and 21075116) and 973 Project (Nos. 2010CB933603 and 2011CB911002).

## Reference

1 M. Grzelczak, J. Vermant, E. M. Furst and L. M. Liz-Marzan, *ACS Nano*, 2010, **4**, 3591–3605.
2 K. J. M. Bishop, C. E. Wilmer, S. Soh and B. A. Grzybowski, *Small*, 2009, **5**, 1600–1630.
3 F. Li, D. P. Josephson and A. Stein, *Angew. Chem., Int. Ed.*, 2011, **50**, 360–388.
4 (*a*) B. Lim, T. Yu and Y. Xia, *Angew. Chem., Int. Ed.*, 2010, **49**, 9819–9820; (*b*) Y. Xia, Y. Xiong, B. Lim and S. E. Skrabalak, *Angew. Chem., Int. Ed.*, 2009, **48**, 60–103; (*c*) S. Guo and S. Dong, *Chem. Soc. Rev.*, 2011, **40**, 2644–2672; (*d*) S. Guo, S. Dong and E. Wang, *Adv. Mater.*, 2010, **22**, 1269–1272; (*e*) S. Guo, S. Dong and

 

E. Wang, *Energy Environ. Sci.*, 2010, **3**, 1307–1310; (*f*) S. Guo, D. Wen, S. Dong and E. Wang, *ACS Nano*, 2010, **4**, 3959–3968; (*g*) S. Guo, S. Dong and E. Wang, *Small*, 2009, **5**, 1869–1876; (*h*) S. Guo, S. Dong and E. Wang, *Chem. Commun.*, 2010, **46**, 1869–1871.
5 L. Wang, Y. Zhu, L. Xu, W. Chen, H. Kuang, L. Liu, A. Agarwal, C. Xu and N. A. Kotov, *Angew. Chem., Int. Ed.*, 2010, **49**, 5472–5475.
6 H. Wang, C. Levin and N. Halas, *J. Am. Chem. Soc.*, 2005, **127**, 14992–14993.
7 X. Zhang, H. Chen and H. Zhang, *Chem. Commun.*, 2007, 1395–1405.
8 A. R. Tao, J. Huang and P. Yang, *Acc. Chem. Res.*, 2008, **41**, 1662–1673.
9 (*a*) Z. Y. Tang, N. A. Kotov and M. Giersig, *Science*, 2002, **297**, 237; (*b*) Z. Y. Tang, Z. L. Zhang, Y. Wang, S. C. Glotzer and N. A. Kotov, *Science*, 2006, **314**, 274.
10 S. Sun, C. B. Murray, D. Weller, L. Folks and A. Moser, *Science*, 2000, **287**, 1989.
11 S. Peng, Y. Lee, C. Wang, H. Yin, S. Dai and S. Sun, *Nano Res.*, 2008, **1**, 229.
12 C. Wang, Y. Hu, C. M. Lieber and S. Sun, *J. Am. Chem. Soc.*, 2008, **130**, 8902–8903.
13 M. Chen, J. Kim, J. P. Liu, H. Fan and S. Sun, *J. Am. Chem. Soc.*, 2006, **128**, 7132–7133.
14 C. Wang, Y. Hou, J. Kim and S. Sun, *Angew. Chem., Int. Ed.*, 2007, **46**, 6333–6335.
15 (*a*) C. Wang, H. Daimon, Y. Lee, J. Kim and S. Sun, *J. Am. Chem. Soc.*, 2007, **129**, 6974–6975; (*b*) C. Wang, H. Daimon, T. Onodera, T. Koda and S. Sun, *Angew. Chem., Int. Ed.*, 2008, **47**, 3588–3591.
16 V. Mazumder, M. Chi, K. L. More and S. Sun, *J. Am. Chem. Soc.*, 2010, **132**, 7848–7849.
17 W. Niu, S. Zheng, D. Wang, X. Liu, H. Li, S. Han, J. Chen, Z. Tang and G. Xu, *J. Am. Chem. Soc.*, 2009, **131**, 697–703.
18 W. Niu, Z. Li, L. Shi, X. Liu, H. Li, S. Han, J. Chen and G. Xu, *Cryst. Growth Des.*, 2008, **8**, 4440–4444.
19 W. Cheng, N. Park, M. T. Walter, M. R. Hartman and D. Luo, *Nat. Nanotechnol.*, 2008, **3**, 682–690.
20 W. Cheng, M. J. Campolongo, S. J. Tan and D. Luo, *Nano Today*, 2009, **4**, 482–493.
21 W. Cheng, M. J. Campolongo, J. J. Cha, S. J. Tan, C. C. Umbach, D. A. Muller and D. Luo, *Nat. Mater.*, 2009, **8**, 519–525.
22 S. Srivastava and N. A. Kotov, *Acc. Chem. Res.*, 2008, **41**, 1831–1841.
23 W. L. Cheng, J. G. Jiang, S. J. Dong and E. Wang, *Chem. Commun.*, 2002, 1706–1707.
24 W. L. Cheng, J. G. Jiang, S. J. Dong and E. Wang, *J. Phys. Chem. B*, 2004, **108**, 19146–19154.
25 L. Deng, Y. Z. Wang, L. Shang, D. Wen, F. A. Wang and S. J. Dong, *Biosens. Bioelectron.*, 2008, **24**, 951–957.
26 Y. Du, C. Chen, J. Yin, B. Li, M. Zhou, S. Dong and E. Wang, *Anal. Chem.*, 2010, **82**, 1556–1563.
27 L. Wang, S. J. Guo, L. J. Huang and S. J. Dong, *Electrochem. Commun.*, 2007, **9**, 827–832.
28 Y. Fang, S. Guo, C. Zhu, Y. Zhai and E. Wang, *Langmuir*, 2010, **26**, 11277–11282.
29 L. H. Zhang, F. Wang and S. J. Dong, *Electrochim. Acta*, 2008, **53**, 6423–6427.
30 X. Hu, W. Cheng, T. Wang, Y. Wang, E. Wang and S. Dong, *J. Phys. Chem. B*, 2005, **109**, 19385–19389.
31 A. To, J. Huang and P. Yang, *Acc. Chem. Res.*, 2008, **41**, 1662–1673.
32 A. Tao, P. Sinsermsuksakul and P. Yang, *Nat. Nanotechnol.*, 2007, **2**, 435–440.
33 H. Song, F. Kim, S. Connor, G. A. Somorjai and P. Yang, *J. Phys. Chem. B*, 2005, **109**, 188–193.
34 A. Tao, F. Kim, C. Hess, J. Goldberger, R. R. He, Y. G. Sun, Y. N. Xia and P. D. Yang, *Nano Lett.*, 2003, **3**, 1229–1233.
35 H. Duan, D. Wang, D. G. Kurth and H. Mohwald, *Angew. Chem., Int. Ed.*, 2004, **43**, 5639–5642.
36 J. Wang, D. Wang, N. S. Sobal, M. Giersig, M. Jiang and H. Mohwald, *Angew. Chem., Int. Ed.*, 2006, **45**, 7963–7966.
37 F. Reincke, S. G. Hickey, W. K. Kegel and D. Vanmaekelbergh, *Angew. Chem., Int. Ed.*, 2004, **43**, 458–462.
38 Y.-J. Li, W.-J. Huang and S.-G. Sun, *Angew. Chem., Int. Ed.*, 2006, **45**, 2537–2539.
39 H. Xia and D. Wang, *Adv. Mater.*, 2008, **20**, 4253–4256.
40 S. J. Guo, S. J. Dong and E. K. Wang, *Cryst. Growth Des.*, 2008, **8**, 3581–3585.
41 S. J. Guo, S. J. Dong and E. K. Wang, *Cryst. Growth Des.*, 2009, **9**, 372–377.
42 H. Wu, F. Bai, Z. Sun, R. E. Haddad, D. M. Boye, Z. Wang, J. Y. Huang and H. Fan, *J. Am. Chem. Soc.*, 2010, **132**, 12826–12828.
43 H. Wu, F. Bai, Z. Sun, R. E. Haddad, D. M. Boye, Z. Wang and H. Fan, *Angew. Chem., Int. Ed.*, 2010, **49**, 8431–8434.
44 A. M. Kalsin, M. Fialkowski, M. Paszewski, S. K. Smoukov, K. J. M. Bishop and B. A. Grzybowski, *Science*, 2006, **312**, 420–424.
45 B. Kowalczyk, D. A. Walker, S. Soh and B. A. Grzybowski, *Angew. Chem., Int. Ed.*, 2010, **49**, 5737–5741.
46 A. M. Kalsin and B. A. Grzybowski, *Nano Lett.*, 2007, **7**, 1018–1021.
47 D. A. Walker, K. P. Browne, B. Kowalczyk and B. A. Grzybowski, *Angew. Chem., Int. Ed.*, 2010, **49**, 6760–6763.
48 (*a*) S. Zhang, X. Kou, Z. Yang, Q. Shi, G. D. Stucky, L. Sun, J. Wang and C. Yan, *Chem. Commun.*, 2007, 1816–1818; (*b*) P. K. Sudeep, S. T. S. Joseph and K. G. Thomas, *J. Am. Chem. Soc.*, 2005, **127**, 6516–6517; (*c*) X. G. Hu, W. L. Cheng, E. K. Wang and S. J. Dong, *Nanotechnology*, 2005, **16**, 2164–2169.
49 Y. Wang, G. Chen, M. Yang, G. Silber, S. Xing, L. H. Tan, F. Wang, Y. Feng, X. Liu, S. Li and H. Chen, *Nature Commun.*, 2010, **1**, 87–93.
50 (*a*) K. K. Caswell, J. N. Wilson, U. H. F. Bunz and C. J. Murphy, *J. Am. Chem. Soc.*, 2003, **125**, 13914–13915; (*b*) J.-Y. Chang, H. M. Wu, H. Chen, Y.-C. Ling and W. H. Tan, *Chem. Commun.*, 2005, 1092–1094; (*c*) M. H. Zareie, X. D. Xu and M. B. Cortie, *Small*, 2007, **3**, 139–145.
51 (*a*) X. Xu, N. L. Rosi, Y. Wang, F. Huo and C. A. Mirkin, *J. Am. Chem. Soc.*, 2006, **128**, 9286–9287; (*b*) M. M. Maye, D. Nykypanchuk, M. Cuisinier, D. van der Lelie and O. Gang, *Nat. Mater.*, 2009, **8**, 388–391; (*c*) J. Sharma, R. Chhabra, Y. Liu, Y. Ke and H. Yan, *Angew. Chem., Int. Ed.*, 2006, **45**, 730–735; (*d*) S. Pal, J. Sharma, H. Yan and Y. Liu, *Chem. Commun.*, 2009, 6059–6061; (*e*) C. Lin, Y. Liu, S. Rinker and H. Yan, *ChemPhysChem*, 2006, **7**, 1641–1647; (*f*) J. Sharma, R. Chhabra, A. Cheng, J. Brownell, Y. Liu and H. Yan, *Science*, 2009, **323**, 112–116.
52 R. Fernandes, M. Li, E. Dujardin, S. Mann and A. G. Kanaras, *Chem. Commun.*, 2010, **46**, 7602–7604.
53 S. Lin, M. Li, E. Dujardin, C. Girard and S. Mann, *Adv. Mater.*, 2005, **17**, 2553–2559.
54 S. Guo, S. J. Dong and E. Wang, *Small*, 2008, **4**, 1133–1138.
55 S. J. Guo, J. Li, W. Ren, D. Wen, S. J. Dong and E. K. Wang, *Chem. Mater.*, 2009, **21**, 2247–2257.
56 S. Guo, S. Dong and E. Wang, *J. Phys. Chem. C*, 2008, **112**, 2389–2393.
57 S. Guo, S. Dong and E. Wang, *Chem.–Eur. J.*, 2009, **15**, 2416–2424.
58 S. Guo, S. Dong and E. Wang, *ACS Nano*, 2010, **4**, 547–555.
59 Y. X. Fang, S. J. Guo, C. Z. Zhu, Y. M. Zhai and E. K. Wang, *Langmuir*, 2010, **26**, 11277–11282.
60 N. Sharma, A. Top, K. L. Kiick and D. J. Pochan, *Angew. Chem.*, 2009, **121**, 7212–7216.
61 S. N. Kim, J. M. Slocik and R. R. Naik, *Small*, 2010, **6**, 1992–1995.
62 W.-Y. Cai, Q. Xu, X.-N. Zhao, J.-J. Zhu and H.-Y. Chen, *Chem. Mater.*, 2006, **18**, 279–284.
63 W. Yang, X. Wang, F. Yang, C. Yang and X. Yang, *Adv. Mater.*, 2008, **20**, 2579–2587.
64 J. Kim, J. E. Lee, J. Lee, Y. Jang, S. W. Kim, K. An, J. H. Yu and T. Hyeon, *Angew. Chem., Int. Ed.*, 2006, **45**, 4789–4793.
65 J. Kim, S. Park, J. E. Lee, S. M. Jin, J. H. Lee, I. S. Lee, I. Yang, J. S. Kim, S. K. Kim, M. H. Cho and T. Hyeon, *Angew. Chem., Int. Ed.*, 2006, **45**, 7754–7758.
66 Y. Jin and X. Gao, *Nat. Nanotechnol.*, 2009, **4**, 571–576.
67 Y. Jin, C. Jia, S.-W. Huang, M. O. Donnell and X. Gao, *Nat. Commun.*, 2010, **1**, 41–48.
68 S. Guo and S. Dong, *TrAC, Trends Anal. Chem.*, 2009, **28**, 96–109.
69 J. Jia, B. Wang, A. Wu, G. Cheng, Z. Li and S. Dong, *Anal. Chem.*, 2002, **74**, 2217–2223.
70 B. K. Jena and C. R. Raj, *Chem.–Eur. J.*, 2006, **12**, 2702–2708.
71 L. Deng, L. Zhang, L. Shang, S. Guo, D. Wen, F. Wang and S. Dong, *Biosens. Bioelectron.*, 2009, **24**, 2273–2276.
72 B. Li, Y. Wang, H. Wei and S. Dong, *Biosens. Bioelectron.*, 2008, **23**, 965–970.
73 L. Wang, T. Li, Y. Du, C. Chen, B. Li, M. Zhou and S. Dong, *Biosens. Bioelectron.*, 2010, **25**, 2622–2626.
74 R. Polsky, R. Gill, L. Kaganovsky and I. Willner, *Anal. Chem.*, 2006, **78**, 2268–2271.

75 Y. Du, B. Li, F. Wang and S. Dong, *Biosens. Bioelectron.*, 2009, **24**, 1979–1983.
76 L. Shen, Z. Chen, Y. Li, S. He, S. Xie, X. Xu, Z. Liang, X. Meng, Q. Li, Z. Zhu, M. Li, X. C. Le and Y. Shao, *Anal. Chem.*, 2008, **80**, 6323–6328.
77 Y.-M. Yan, R. T. Vered, O. Yehezkeli, Z. Cheglakov and I. Willner, *Adv. Mater.*, 2008, **20**, 2365–2370.
78 M. Riskin, R. T. Vered and I. Willner, *Adv. Mater.*, 2010, **22**, 1387–1391.
79 I. Willner and B. Willner, *Nano Lett.*, 2010, **10**, 3805–3815.
80 T. Niazov, V. Pavlov, Y. Xiao, R. Gill and I. Willner, *Nano Lett.*, 2004, **4**, 1683–1687.
81 Y. Du, C. Chen, M. Zhou, S. Dong and E. Wang, *Anal. Chem.*, 2011, **83**, 1523–1529.
82 X. Sun, Y. Du, S. Dong and E. Wang, *Anal. Chem.*, 2005, **77**, 8166–8169.
83 X. Sun, Y. Du, L. Zhang, S. Dong and E. Wang, *Anal. Chem.*, 2006, **78**, 6674–6677.
84 Y. Du, B. Qi, X. Yang and E. Wang, *J. Phys. Chem. B*, 2006, **110**, 21662–21666.
85 J. P. Camden, J. A. Dieringer, J. Zhao and R. P. Van Duyne, *Acc. Chem. Res.*, 2008, **41**, 1653–1661.
86 L. Lu and A. Eychmüller, *Acc. Chem. Res.*, 2008, **41**, 244–253.
87 X. Zou and S. Dong, *J. Phys. Chem. B*, 2006, **110**, 21545–21550.
88 Z. Zhu, H. Meng, W. Liu, X. Liu, J. Gong, X. Qiu, L. Jiang, D. Wang and Z. Tang, *Angew. Chem., Int. Ed.*, 2011, **50**, 1593–1596.
89 G. Braun, S. J. Lee, M. Dante, T.-Q. Nguyen, M. Moskovits and N. Reich, *J. Am. Chem. Soc.*, 2007, **129**, 6378–6379.
90 Y. Wang, H. Wei, B. Li, W. Ren, S. Guo, S. Dong and E. Wang, *Chem. Commun.*, 2007, 5220–5222.
91 L. Fabris, M. Dante, T.-Q. Nguyen, J. B.-H. Tok and G. C. Bazan, *Adv. Funct. Mater.*, 2008, **18**, 2518–2525.
92 L. Fabris, M. Schierhorn, M. Moskovits and G. C. Bazan, *Small*, 2010, **6**, 1550–1557.
93 Y. Wang, K. Lee and J. Irudayaraj, *Chem. Commun.*, 2010, **46**, 613–615.
94 Y. Wang and J. Irudayaraj, *Chem. Commun.*, 2011, **47**, 4394–4396.
95 H. Cho, B. R. Baker, S. Wachsmann-Hogiu, C. V. Pagba, T. A. Laurence, S. M. Lane, L. P. Lee and J. B.-H. Tok, *Nano Lett.*, 2008, **8**, 4386–4390.
96 J.-W. Chen, X.-P. Liu, K.-J. Feng, Y. Liang, J.-H. Jiang, G.-L. Shen and R.-Q. Yu, *Biosens. Bioelectron.*, 2008, **24**, 66–71.




 